

Honors Thesis

Reagan Goodwin

05/20/21

Intraflagellar transport is not required for flagellar associated protein 93 (FAP93) assembly in *Chlamydomonas reinhardtii* cilia.

Abstract

Eukaryotic cilia are essential organelles that are found on the surface of most differentiated cells in the human body. Defects associated with ciliary assembly and function can lead to a wide array of diseases termed ciliopathies. This highly conserved organelle is comprised of over 650 proteins that are precisely arranged in a repetitive pattern along the length of the cilium. Various model organisms have been utilized to elucidate the assembly mechanisms of these proteins, but many remain unknown. One evolutionarily conserved mechanism of assembly is intraflagellar transport (IFT) which uses molecular motors and associated proteins to deliver ciliary components from the cell body. The work presented here uses the genetic model organism *Chlamydomonas reinhardtii* to investigate the mechanism of assembly of the proximally localized FAP93 protein. To test the hypothesis that FAP93 uses IFT to assemble on the cilium, dikaryon rescue is performed using a conditional IFT mutant to observe FAP93 assembly when IFT is functional and nonfunctional. Results from this research indicate that FAP93 does not require IFT to assemble in the cilium. Thus, FAP93 likely enters the cilium via diffusion to assemble in the cilium or requires accessory proteins to be transported using IFT.

Introduction

Eukaryotic cilia, also termed flagella, are organelles that are essential for signaling and motility (Baker and Beales, 2007). Cilia are antennae like structures that protrude from the cell body on various cell types and can be either non-motile or motile; non-motile primary cilia are associated with cell signaling while motile cilia are associated with fluid flow and motility (Van der Heiden et al., 2011). Cilia are found on most differentiated cells in the human body; you can find them in the brain, airways, and reproductive systems (Ringers et al., 2020). Cilia play various roles depending upon where they are located, in the brain these organelles move cerebrospinal fluid, in airways they clear debris to prevent infections, and during development they direct left and right patterning which dictates the body plan. Defects in genes associated with ciliary assembly have been linked to various diseases termed ciliopathies (reviewed in Fliegauf et al., 2007; Lewis et al., 2016; Brown and Witman, 2014). These ciliopathies include, but are not limited to, hydrocephalus, retinal degeneration, situs inversus, and infertility. Defects in cilia can be particularly detrimental to an organism due to their ubiquitous presence in various cell types, and ciliary research is vital to determining the specific genetic defects associated with ciliopathies (Brown and Witman, 2014; Wang and Dynlacht, 2018).

The motile eukaryotic cilium is an evolutionarily conserved structure found in various organisms such as mice, sea urchins, and tetrahymena (Pazour et al., 2000; Pigino et al., 2012). It is highly complex and ordered, encompassing over 650 unique proteins for its assembly and function (Pazour et al., 2000; Nicastro 2007; Nicastro et al., 2009). The motile eukaryotic cilium is comprised of a core microtubule (MT)-based axoneme that includes a central pair (CP) of microtubules that are enclosed by a circle of nine doublet microtubules (DMT), this structure is referred to as the 9 + 2 axoneme (Fig. 1A; Porter and Sale, 2000). Along the length of the cilium,

there is a repeating set of proteins and structures that occur every 96nm, which is the basis for the periodicity of the cilium (Fig. 1B; Oda et al., 2014; Nicastro et al., 2006). For each 96nm repeat there are two radial spokes (RS) that extend from the outer doublet microtubules (DMT) to a central pair of singlet microtubules (CP). Molecular motors that drive motility, inner and outer dynein arms (IDAs) (ODAs), are located on the DMTs; there are seven distinct IDAs and four identical ODAs per 96nm repeat (Fig. 1B; King and Sale, 2018, Nicastro et al., 2006). The axoneme is comprised of various other proteins and protein complexes associated with the 9+2 axonemal structure, some of which are found along the entire length while others are localized to a specific region of the axoneme (Alford et al., 2013).

In addition to the repeating set of proteins and structures that occur every 96nm along the length of the cilium, some proteins are assembled at a specific location on the cilium (Bui et al., 2012; Hoops and Witman, 1983; Piperno and Ramanis, 1991). Tubulin, radial spokes, and the outer dynein arms are examples of proteins found in each 96nm repeat (Fig. 1B) throughout the cilium. In contrast, there are some proteins localized to particular regions of the cilium. For example, the proximal end of the cilium has specialized IDAs, similar to the IDAs along the rest of the cilium and an end-binding protein 1 (EB1) that is localized to the ciliary tip (Bui et al., 2012; Piperno and Ramanis, 1991; Hoops and Witman, 1983; Harris et al., 2016). Recent technological advancements have significantly increased the amount of knowledge on eukaryotic cilia, however there is still much that remains unknown about the mechanism of assembly of these various proteins and why some are localized to specific regions on the cilium.

Axonemal proteins are synthesized in the cell body because the cilium does not have ribosomes, therefore all proteins and protein complexes that are made in the cell need to travel from the cell body into the cilium. For example, radial spokes, dynein arms, central pair proteins

and even tubulin are made in the cell and transported into the cilium (Diener, 2009; Viswanadha et al., 2014; Hunter et al., 2018). One mechanism for transporting these complexes to the cilium is intraflagellar transport (IFT; Rosenbaum et al., 1999; Diener, 2009; Lecktreck et al., 2015). IFT is the bidirectional transport of particles in the cilium; the anterograde direction is from the cell body to the tip of the cilium and retrograde refers to movement from the distal tip to the base of the cilium (Kozminski et al., 1993; Pigino et al., 2009). IFT was first visualized in *C. reinhardtii* (Kozminski et al., 1993) and this mechanism of transport is highly conserved structurally and functionally; it can be found in *C. elegans*, tetrahymena, and mammals (Rosenbaum and Witman, 2002).

The anterograde movement of proteins is powered by heterotrimeric kinesin-II and the retrograde movement is powered by cytoplasmic dynein 1b (Fig. 2A; Cole, 1998; Rosenbaum and Witman, 2002, Webb et al., 2020). Kinesin-II and dynein 1b are motor proteins that move along the outer DMTs powered by ATP hydrolysis. These molecular motors bind to IFT particles (Fig. 2A and B) which are made from two complexes termed IFT complex A and B, simplified as an IFT particle in figure 2. (Stepanek and Pigino, 2016). Complex A has been associated with six subunits, but it is unknown if every complex will have all six subunits, (Cole et al., 1998; Piperno et al., 1998; Pazour et al., 2000) and complex B has been associated with 14 subunits (Cole et al., 1998; Luckner et al., 2005). Some subunits in complex A and B bind to specific cargo but there are multiple binding sites that allow for IFT particles to bind to multiple cargo and their motor protein, forming an IFT train or raft (Fig. 2B; Cole, 2003; Taschner and Lorentzen, 2016).

Most of what we know about IFT comes from studies utilizing the model organism *Chlamydomonas reinhardtii* (Cole et al., 2003). *C. reinhardtii* has been widely used to study ciliary assembly and associated proteins (Salome and Merchant, 2019). This genetic model

organism is a single-celled eukaryote; it is a species of green algae and possesses two motile cilia (Tran, 2020). This model organism has been a key genetic tool in investigating cilia due to the large collection of mutants, simple cell culture maintenance, ease of observation using a microscope, and the cells are excellent for obtaining large amounts of cilia (Silflow and Lefebvre, 2001). Cilia are also studied in other model organisms such as *C. elegans*, xenopus, and mice (Ostrowski et al., 2011), but *C. reinhardtii* is the best model organism for my particular project because of available mutants and genetic techniques that are specific to the organism (Gibbons, 1981; Pigino et al., 2012; Dutcher. 2014; Silflow and Lefebvre, 2001).

Using *C. reinhardtii*, previous data show that the flagellar associated protein 93 (FAP93) is enriched in short axonemes and is localized to the proximal end of the cilium, near the cell body; however, the function of this protein is unknown (Huang et al., manuscript in preparation). The FAP93 protein is 671 amino acids in length and estimated to be 260 kilodaltons. Additionally, FAP93 is an intrinsically disordered protein with a coiled-coil domain and several stretches of repetitive amino acids. There are partial orthologs in species such as *Volvox carteri*, *Paramecium tetraurelia*, and *Caenorhabditis tropicalis* (Szklarczyk et al., 2018). In order to decipher the function of FAP93, I aim to determine its mechanism of assembly. I hypothesize that FAP93 uses intraflagellar transport to enter and be deposited for assembly on the proximal axonemal microtubules. Alternatively, FAP93 may enter the cilia independent of IFT. My experiment was designed to distinguish these mechanisms for FAP93 transport and possibly reveal novel mechanisms for ciliary assembly.

In order to test the hypothesis that FAP93 is assembled on the axoneme via IFT, I used the conditional *C. reinhardtii* mutant *fla10-1*. This mutant allows for the investigation of assembly of various proteins along the axoneme and has been used to study IFT and the cargo

that is being transported into the cilium (Hunter et al, 2018; Viswanadha et al., 2014). This mutant is widely used for investigating the assembly of proteins via IFT, because the *fla10-1* mutant is temperature sensitive, meaning it has functional IFT at a permissive temperature (21°C) and defective IFT at a restrictive temperature (32°C). The defect in this mutant is a cytosine to adenine transversion at amino acid 329 in the motor domain. This single change affects the kinesin-homologous protein 1, (KHP1) which is a subunit of kinesin-II (Walther et al., 1994). Kinesin-II is required for anterograde IFT, and this mutation does not affect the protein at the permissive temperature, but causes it to be dysfunctional at the restrictive temperature (Piperno et al., 1996).

In this study the *fla10-1* mutant is used in dikaryon rescue, a technique that results in cytoplasmic complementation (Dutcher, 2014). Dikaryon formation occurs by mating two gametic cells of opposite mating type resulting in a temporary quadra-ciliated cell with two nuclei and common cytoplasm of both cells (Fig. 3). The two cell types to be mated in the work presented here are *fla10-1* and the double mutant *fap93;fla10-1*. These two mutants are used because the resulting dikaryon cell will have two copies of the temperature sensitive gene *FLA10*, a wild-type copy of *FAP93*, and a defective copy of *FAP93* (Fig. 3). When the two cell types fuse into one cell, cytoplasmic complementation occurs and the proteins and genes in one cell are now available to the other. This unique technique in *C. reinhardtii* allows us to visualize the recovery of proteins in a cilia from the cell that was previously deficient in that protein (see Dutcher, 2014). Specifically, the *fla10-1* cell has a fully assembled FAP93 region at the proximal axoneme and the *fap93;fla10-1* initially does not assemble FAP93 in the otherwise fully assembled cilium (Fig. 3). When the two cells fuse at the permissive temperature, the resulting quadra-ciliated cell is expected to rescue FAP93 assembly in the cilium missing FAP93, thus all

four cilia will have FAP93. This control experiment will indicate rescue has occurred in the *fap93;fla10-1* cilia (Fig. 3) and the dikaryon formed at the restrictive temperature will indicate if FAP93 is using IFT to assemble.

Results

Characterization of fla10-1 and fap93;fla10-1 mutants

The presence or absence of FAP93 in the *fla10-1* cells was confirmed by immunofluorescence microscopy. An antibody against acetylated tubulin was utilized to mark axoneme and a specific FAP93 antibody was utilized to confirm FAP93 presence or absence. The *fla10-1* mutant has FAP93 on both cilia (Fig. 4). This confirms that the *fla10-1* has FAP93 and the *fla10-1* cilia (11.24 ± 1.89) were comparable in ciliary length to wild type (11.21 ± 1.74) under normal conditions. The FAP93 domain of *fla10-1* (0.89 ± 0.31) is smaller than wildtype (1.35 ± 0.22).

After 90 minutes *fla10-1* cilia should shorten approximately 20% because anterograde IFT ceases when the kinesin-2 motor is defective (Kozminksi et al., 1995). To confirm the *fla10-1* cells have the defective kinesin at the restrictive temperature of 32°C, I performed an immunofluorescence after allowing the cells to incubate at the permissive or restrictive temperature for two hours. In this experiment CC125 was utilized as a comparison to observe shortening of the cilia (Fig. 5). The *fla10-1* cilia at the permissive temperature (21°C) are equivalent to CC125, *fla10-1* at the restrictive temperature (32°C) show shorter cilia in comparison to the wild type at both conditions and the *fla10-1* at permissive (fig. 5). This result confirms that the *fla10-1* cells have defective kinesin-2 and IFT at the restrictive temperature.

Similarly in the *fap93;fla10-1* mutant, the absence of FAP93 was confirmed by immunofluorescence microscopy. The *fap93;fla10-1* mutant lacks FAP93 staining on both cilia (Fig. 4), confirming that the *fap93;fla10-1* mutant is missing FAP93. The *fap93;fla10-1* cilia (9.93 ± 1.27) are shorter than wild type cilia.

Additionally, the *FLA10* defect was confirmed in the *fap93;fla10-1* mutant. The same experiment was performed as stated in the *fla10-1* characterization, however the cells were visualized via phase contrast (Fig. 6). The *fap93;fla10-1* mutant shows shortening of the cilia at the restrictive temperature, confirming that it also has the temperature sensitive *FLA10* mutation.

Dikaryon Rescue of FAP93 at permissive and restrictive temperatures

To determine if FAP93 requires IFT for assembly, dikaryons between *fla10-1* and *fap93;fla10-1* were generated at the permissive temperature of 21°C and the restrictive temperature of 32°C to observe rescue of the FAP93 protein. Cells were allowed to mate for 30 minutes, because at this time point I saw the highest quantity of dikaryons formed. Dikaryons were identified by the presence of four cilia on one cell. In this experiment, the wild-type copy of FAP93 from *fla10-1* is expected to rescue FAP93 assembly in the *fap93;fla10-1* cilium. Rescue will be confirmed by the presence of FAP93 on all four cilia. For example, other cell components like the II dynein and axonemal components like the DRC can be rescued with this method at the permissive temperature when IFT is functional (Viswanadha et al., 2015; Wren et al., 2013).

To observe the cilia and FAP93 protein, I performed an immunofluorescence microscopy on dikaryons at both the permissive and restrictive temperatures. The cilium will be visualized with a monoclonal antibody against acetylated tubulin which is specific to axonemal tubulin and

shows the full length of the cilia; an anti-mouse secondary antibody will show the cilium in red. A rabbit polyclonal antibody against FAP93 will be used to visualize FAP93 using an anti-rabbit secondary antibody in green (Fig. 3, 7, and 8).

When the cells are mated at the permissive temperature, FAP93 is expected to be seen in all four cilia (Fig. 3, 7A). At the restrictive temperature of 32°C, the FLA10 protein is not functional which results in defective IFT. If FAP93 assembly is independent of IFT, then all four dikaryon cilia are expected to contain FAP93 at the proximal end (Fig. 7B). If FAP93 requires IFT for assembly on the axoneme, then in the dikaryons formed at the restrictive temperature FAP93 staining should only be localized to two cilia originally from the *fla10-1* cell (Fig. 7C). At the permissive temperature of 21°C, FAP93 is localized to the proximal end of all four cilia in the dikaryons (Fig. 8 a-c). This result indicates the *fla10-1* and *fap93;fla10-1* cells are compatible for mating and FAP93 can be rescued using this technique when IFT is on. Similarly, dikaryons formed at the restrictive temperature of 32°C when IFT is off show FAP93 is localized to the proximal end of all four cilia (Fig. 8 d-f). This result indicates FAP93 rescue, identical to the dikaryons formed at the permissive temperature, which in return suggests FAP93 does not require IFT for assembly.

The length analysis of the dikaryons cilia and FAP93 regions indicate there is no significant difference between the dikaryons at these two conditions. Dikaryon ciliary length at 21°C was 9.55µm (±1.27µm), similarly at 32°C ciliary length was 9.83µm (±1.13µm)(Fig. 9, black bars). The FAP93 region from the *fla10-1* cilia at 21°C was 0.99µm (±0.23µm) and 1.05µm (±0.21µm) at 32°C (Fig. 9, grey bars).

Interestingly, partial rescue of FAP93 was observed at both conditions. The rescued FAP93 regions at both conditions are significantly shorter in length in comparison to the FAP93

region in *fla10-1* cilia (Fig. 8 arrow head). The *fap93;fla10-1* FAP93 region or rescued region at 21°C was 0.42µm (±0.10µm) and 0.45µm (±0.18µm) at 32°C (Fig. 9, white bars). The lack of differences between the dikaryons at these conditions suggest that IFT is not playing a role in the assembly of FAP93, and it is interesting to see consistent partial recovery at both conditions.

Discussion

Cilia play a vital role in various cellular processes in a variety of organisms, making them an important area of research (reviewed in Fliegauf et al., 2007; Lewis et al., 2016; Brown and Witman, ;Wallmeier et al., 2020). There are still a considerable number of gaps in knowledge about ciliary assembly, specifically the roles of adapter proteins and alternatives to IFT like diffusion. Here, the mechanism of assembly for the FAP93 protein was investigated and found to be independent of IFT. Identifying the mechanism of assembly for various proteins allows us to investigate various methods of assembly and discover common factors required for ciliary assembly.

For my research, I hypothesized that FAP93 utilizes IFT to assemble on the axoneme, similar to many axonemal proteins (Hunter et al., 2018; Viswanadha et al., 2014; Wren et al., 2013). By using the *fla10-1* temperature sensitive mutant, I found that FAP93 does not require IFT to assemble, contrary to what was hypothesized. Assembly of the protein on the cilia that were previously lacking FAP93 at the proximal end constitutes rescue. Results from the dikaryon rescue at the restrictive temperature suggest that FAP93 does not require IFT to assemble on the axoneme. Interestingly, FAP93 in recovering *fap93;fla10-1* cilia is identical at permissive and restrictive temperatures, suggesting that the presence of IFT does not influence the recovery of FAP93. Although IFT is a common mechanism of ciliary assembly, there are proteins that do not completely require IFT to assemble, which supports the prospect of FAP93 utilizing a different

mechanism of assembly (Craft et al., 2015; Craft et al., 2020). Another example, the plus-end binding protein 1 (EB1) assembles independently of IFT and transport occurs by diffusion (Harris et al., 2016). One surprising result was the partial rescue of FAP93 at both temperatures in the dikaryon experiment, this is shown in Figure 8 (smaller region denoted by arrow). Partial recovery of FAP93 is indicated by two wild-type FAP93 regions and two reduced FAP93 regions. There are several possible explanations for partial rescue, this could be a result of slow assembly, availability of the protein in the cell, or an interesting alternative would be FAP93 requires an accessory protein for transport or docking on the axoneme.

Again since IFT is not being utilized, FAP93 is potentially assembling on the cilium via diffusion, which may account for the partial recovery of FAP93. Tubulin utilizes IFT to assemble, however when IFT is nonfunctional it can still assemble in the axoneme via diffusion in smaller amounts. The partial recovery may be due to a slow diffusion rate, and live cell imaging would be required to determine if FAP93 is diffusing into the cilium, additionally this experiment could provide more information on the rate of FAP93 diffusion.

Alternatively, there may be an accessory protein that FAP93 requires for full assembly or a preassembled structure could prevent the complete recovery. If there is a protein or structure that is preventing FAP93 from diffusing fully into the normal FAP93 region, this blockage does not occur in growing cilia, because all the proteins and structures would be assembling at the same time. In the dikaryon experiment, the cilium is already built when the new FAP93 is introduced and because of the previous lack of FAP93, there might be another protein that bound where FAP93 is localized. Performing a dikaryon rescue followed by deciliation would allow FAP93 to assemble concurrently with the rest of the ciliary proteins (Fig.10). This additional experiment would test the hypothesis that FAP93 is not fully recovering to due a required

accessory protein or there is a protein or structure blocking its entry to the normal region. In this experiment, dikaryons at the restrictive temperature would not be expected to regenerate cilia because IFT is off and this would serve as an internal control. The dikaryons that are deciliated at the permissive temperature would be allowed to regrow and then cells would be visualized via immunofluorescence. Two possible results are shown in Figure 10, in A there may be full recovery of FAP93 which would be indicated by four equal FAP93 regions that are comparable to the *fla10-1* FAP93 regions. Alternatively in B, partial rescue may be observed, this would be indicated by four reduced FAP93 regions on all four cilia. This result would suggest either there is not enough FAP93 protein available for assembly or the protein assembles slower than the rest of the cilium, possibly because of diffusion.

The data presented here supports that FAP93 does not use IFT to assemble on the axoneme, contrary to the proposed hypothesis. Further studies are required to elucidate the mechanism of FAP93 assembly and the cause of the partial recovery of the FAP93 protein. Performing the additional dikaryon deciliation or live cell imaging experiments will offer more insight into how FAP93 is assembling on the axoneme and could potentially assist in identifying accessory proteins that FAP93 requires to assemble. This work has further characterized the FAP93 protein by determining that it does not require IFT for axonemal assembly. These data can inform future studies aimed towards deciphering the role of FAP93.

Figures

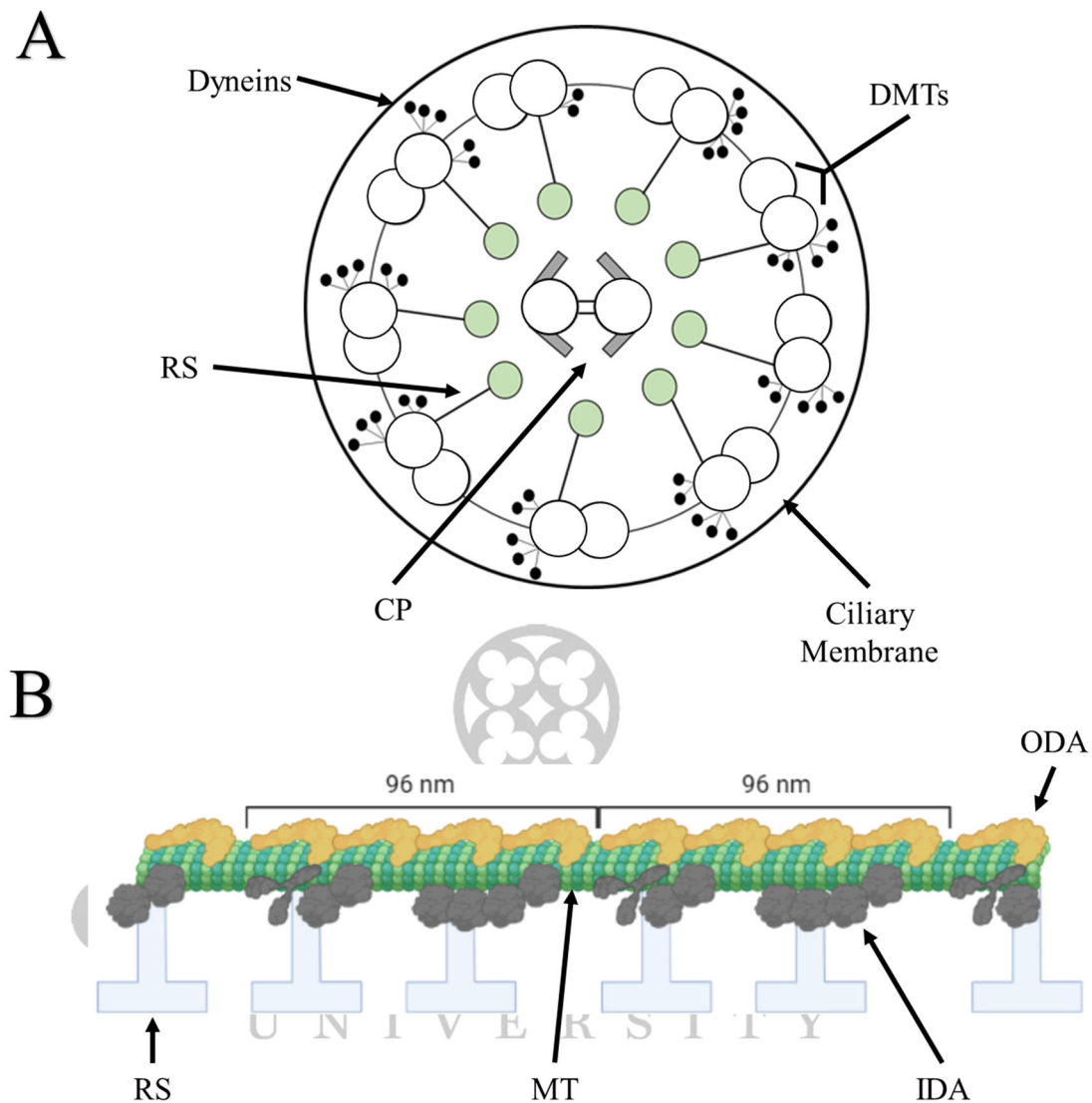


Figure 1. Molecular Structure of Motile Cilia. (A) Schematic diagram of a cross section of the cilium. The outer ring is the ciliary membrane, DMT are the nine doublet microtubules, CP is the central pair, RS is the radial spokes, and dyneins are located on the outside and inside of the DMTs. (B) Longitudinal view of a microtubule doublet. The orange densities depict the four outer dynein arms (ODAs) that power ciliary movement, grey densities depict the seven inner dynein arms (IDAs) that generate ciliary bends for movement, blue t-shaped structures are the

radial spokes (RS) that allow the CP to communicate to the ODMTs and regulate dynein activity, and all structures shown are bound to the ODMT in green and blue. This structure repeats every 96nm and serves as a molecular ruler for the cilium.

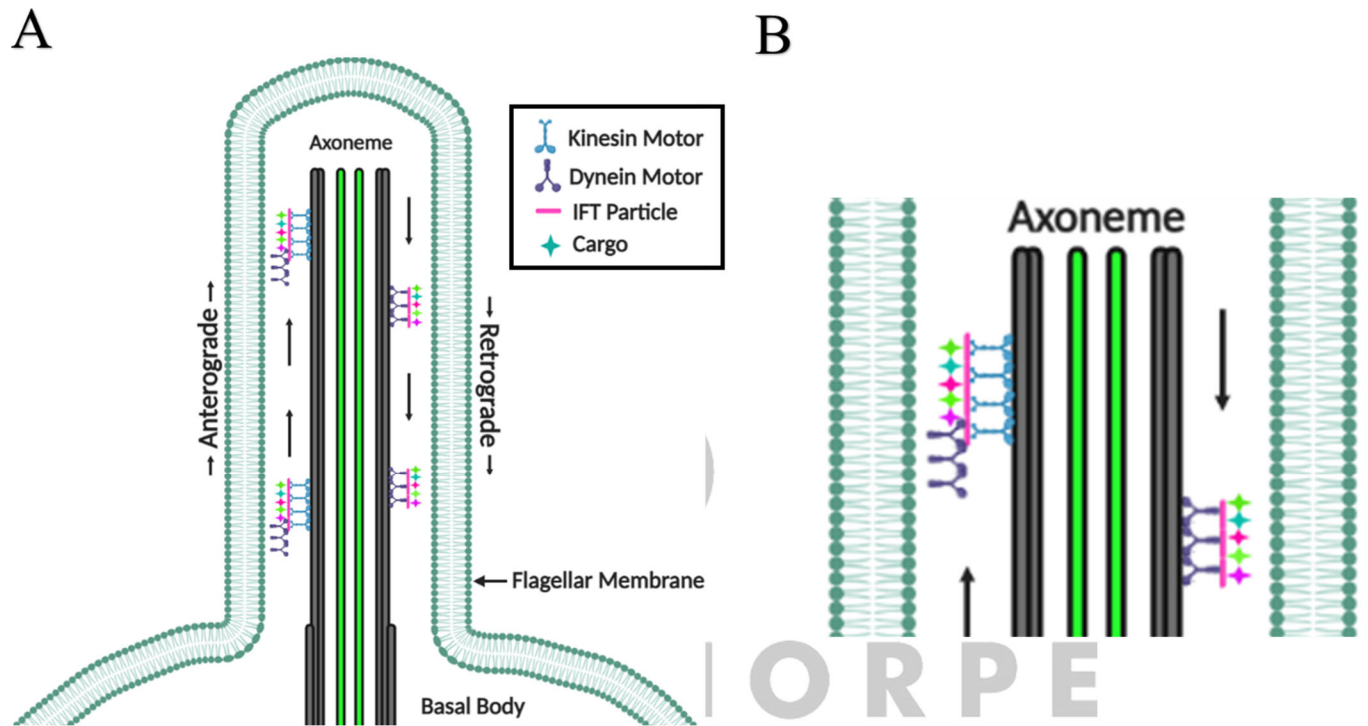


Figure 2. Schematic Diagram of Intraflagellar Transport Machinery. (A) The longitudinal schematic of the cilium depicts the structure of the core axoneme with the cell body at the bottom of the image with the cilium protruding from the surface of the cell. The flagellar membrane is continuous from the cellular membrane and shown in blue. In the center of the diagram the central pair MTs are shown in green and the outer doublet microtubules (ODMTs) are black. Intraflagellar transport (IFT) machinery is depicted between the outer doublet microtubules and the flagellar membrane. The kinesin motors (blue) are located on the left of the ODMTs driving IFT's anterograde motion and dynein motors (purple) are located to the right of ODMTs driving IFT's retrograde motion. The IFT components are referred to as an IFT train,

the train consists of the molecular motor, IFT particles, and the cargo. The molecular motors bind to IFT particles (pink) and their corresponding cargo (multicolored stars). The cargo is depicted in various colors because there is a wide range of potential cargos that are transported via IFT (image created in biorender). The molecular motors “walk” along the MTs in their respective directions, and they are powered by ATP hydrolysis. On the right (**1B**) an enlarged section of the axoneme depicts the IFT machinery (image created in biorender). On the kinesin motor (blue) there are two small subunits that attach to the MT and walk along the MT, one of the subunits is FLA10.

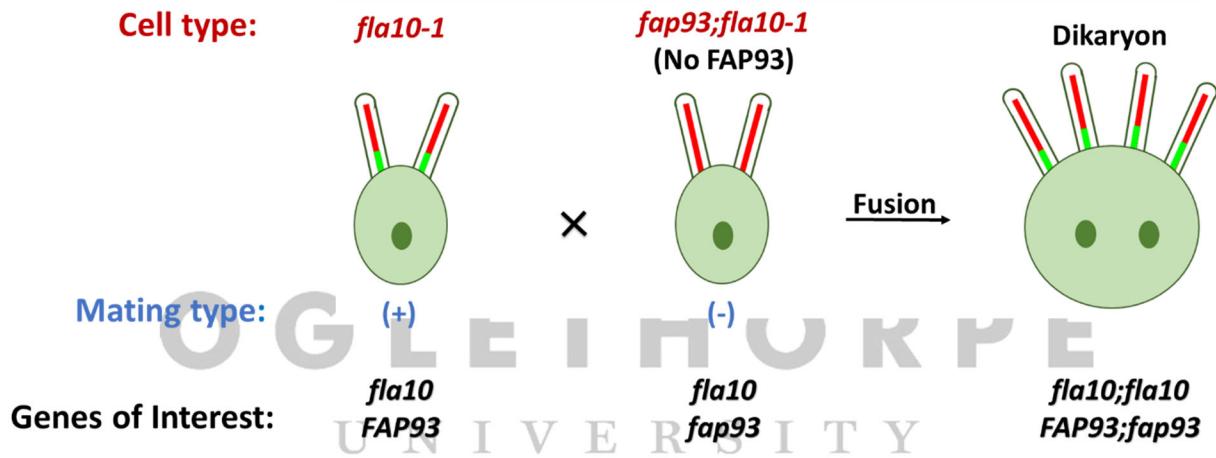


Figure 3. Dikaryon Rescue in *Chlamydomonas reinhardtii*. *Fla10-1* (mating type (+)) and *fap93;fla10-1* (mating type (-)) are cultured separately in media that lacks nitrogen to differentiate the cells into gametes so the mating can occur. When the cells are combined, fusion will occur forming a single cell, that contains both nuclei, shared cytoplasm, and four cilia, termed a dikaryon. The *fla10-1* cell has a defective copy of the *FLA10* gene and a wild-type copy of the *FAP93* gene. The FAP93 protein is depicted as the green region at the base of the cilia. The *fap93;fla10-1* double mutant cell has a defective copy of the *FLA10* and *FAP93* gene, thus the FAP93 protein is absent in the cell, which is indicated by the lack of green at the

proximal end. The prediction is that when these cells form a dikaryon the cell will have two copies of the defective *FLA10* gene and one wild-type copy of *FAP93* which will rescue the defective copy at permissive temperature and the FAP93 protein will be assembled in all four cilia.

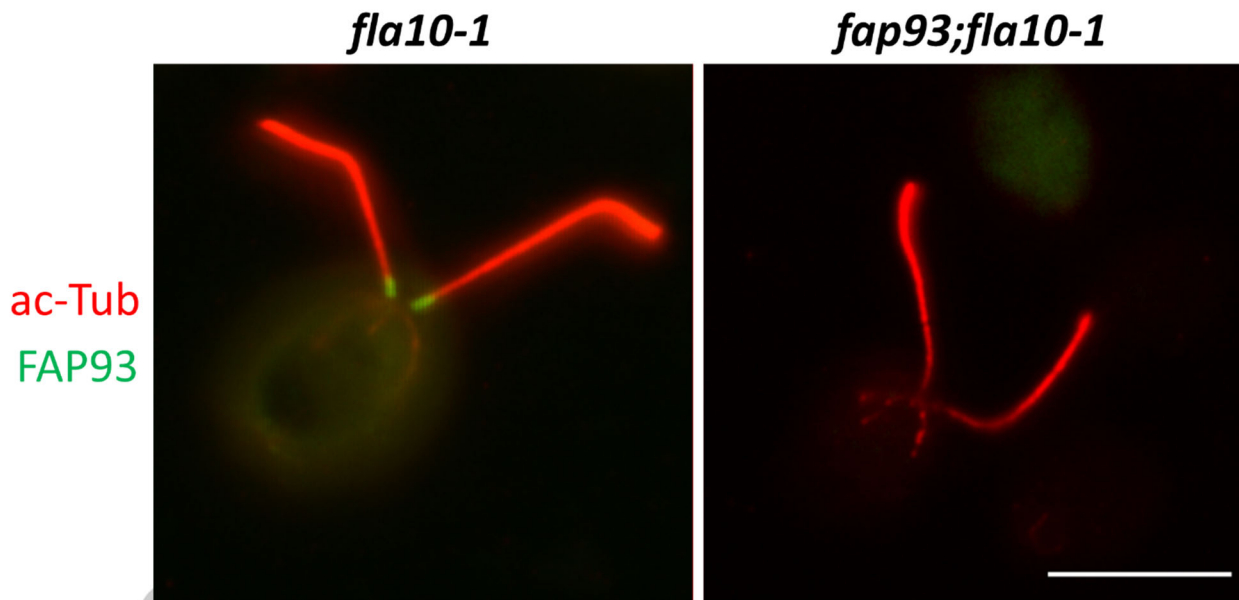


Figure 4. FAP93 is present on *fla10-1* but absent from *fap93;fla10-1* axonemes. Acetylated tubulin (ac-Tub) is shown in red using a primary mouse monoclonal antibody 611B1 and secondary antibody conjugated to anti-mouse-555. Ac-Tub depicts the length of the cilia. FAP93 localization is shown in green using a rabbit polyclonal antibody to FAP93 and an anti-rabbit-488 secondary antibody. The *fla10-1* cell on the left shows two FAP93 stains at the base of the cilium, indicating it has FAP93. The *fap93;fla10-1* cell on the right has no FAP93 staining, indicating it is deficient in FAP93. (Scale bar = 10 μ m).

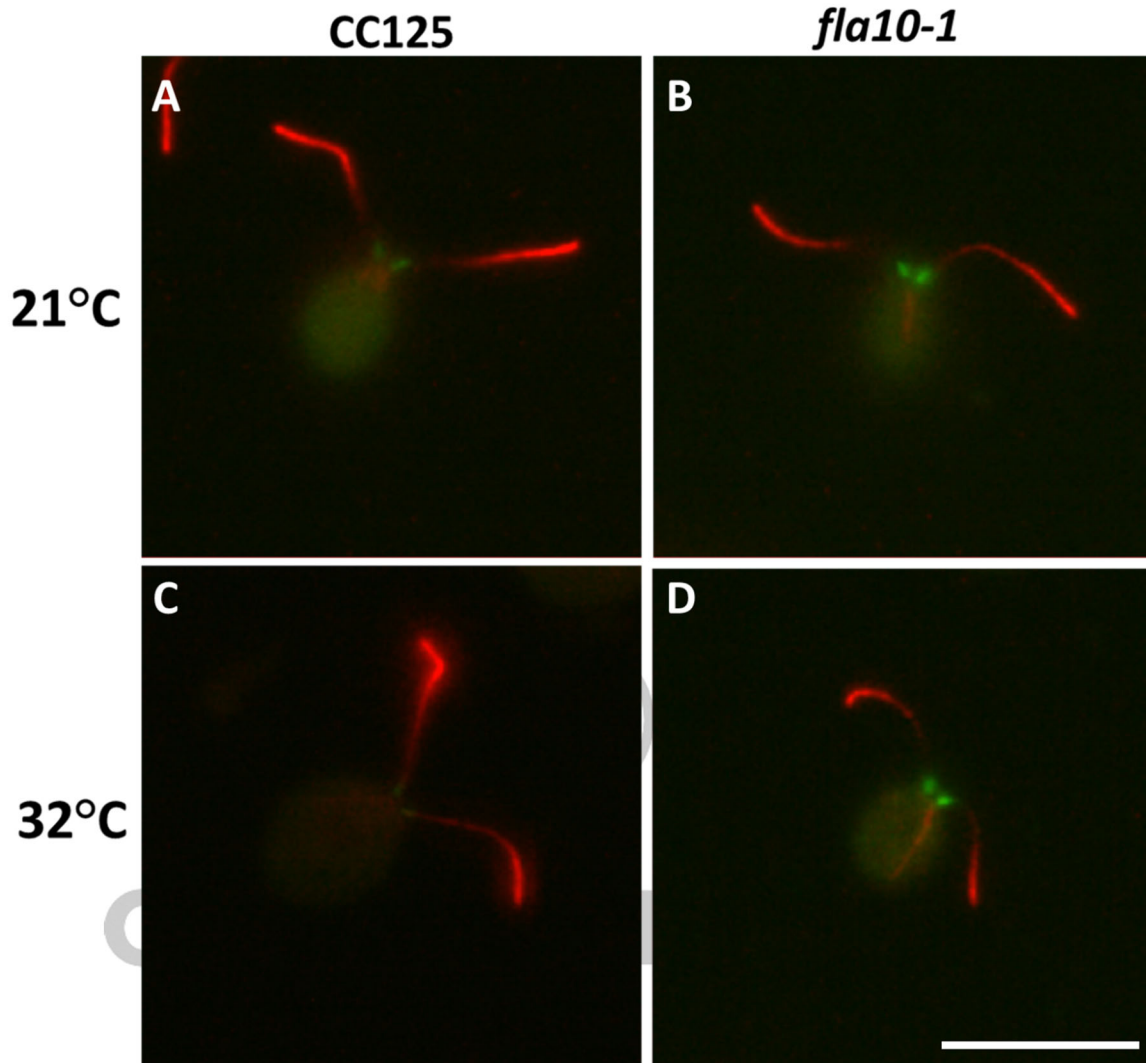


Figure 5. *fla10-1* cilia shorten at the restrictive temperature. The first column depicts the wild type strain CC125 (A, C) and the secondary column shows *fla10-1* (B, D). In A and B the cells are at the permissive temperature of 21°C, when IFT is on and *fla10-1* is like wild-type. In C and D the cells are at the restrictive temperature of 32°C, when *fla10-1* cilia should shorten in length because IFT is off. Cells were kept at their respective temperature for two hours in L media before immunofluorescence. Acetylated tubulin (ac-Tub) is shown in red using a primary mouse monoclonal antibody 611B1 and secondary conjugated to anti mouse-555. Ac-Tub depicts length of the cilia. FAP93 localization is shown in green using a rabbit polyclonal

antibody to FAP93 and an anti-rabbit secondary antibody conjugated to anti-rabbit-488. (Scale bar = 10 μ m).

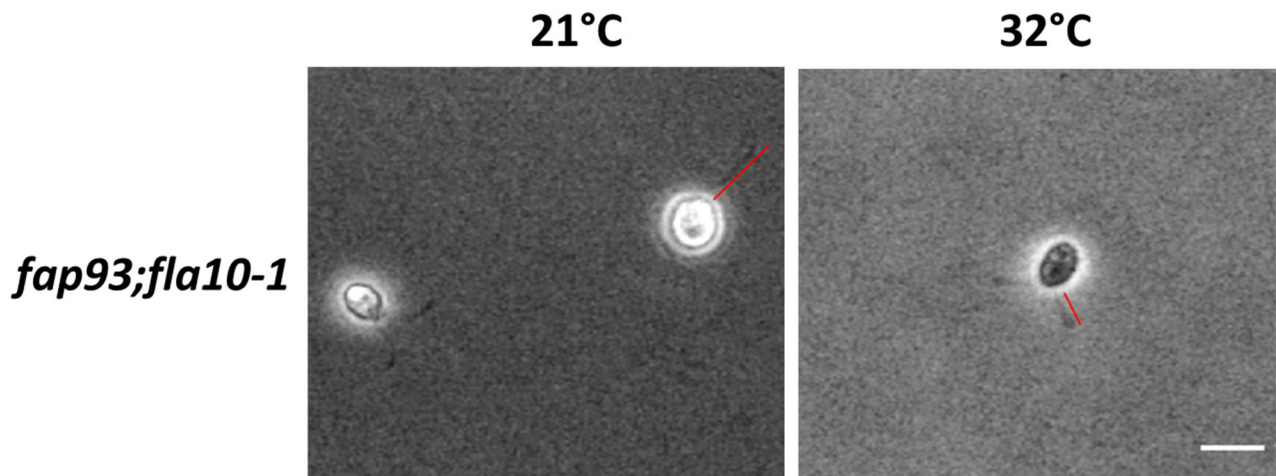


Figure 6. *fap93;fla10-1* cilia shorten at the restrictive temperature. Cells were incubated at either 21°C or 32°C for two hours in L media. Cells were then visualized via light microscopy with formaldehyde. The panel on the left are the *fap93;fla10-1* cells at the permissive temperature, cilia should be full length indicated by the redline. On the right panel, the cells are at the restrictive temperature and should be shorter because IFT is off. The cilia are shorter and their length is shown by the red line. (Scale bar = 10 μ m).

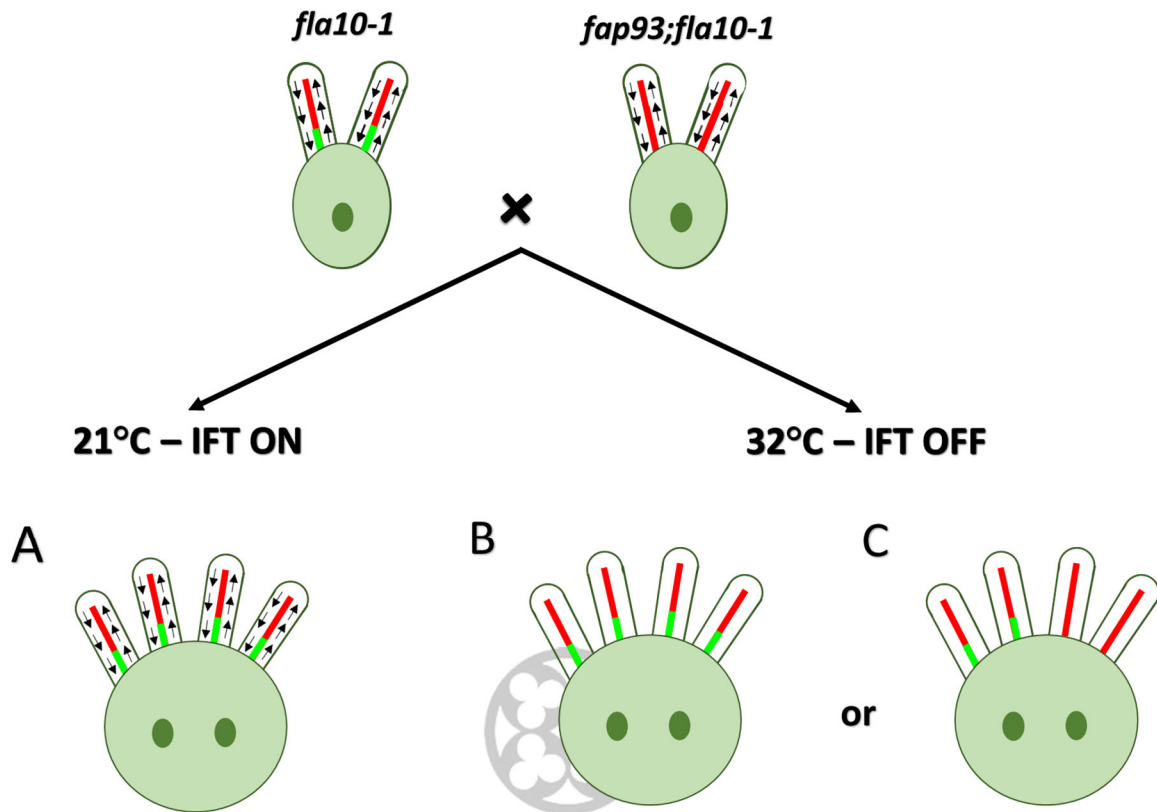


Figure 7. Experimental design of dikaryon rescue with the *fla10-1* mutant. The predicted outcomes of the dikaryon rescue described in **Figure 3** are shown here. Nitrogen starved cells are preincubated at either permissive (21°C) or restrictive (32°C) temperatures for 20 minutes. The dikaryons are then examined by immunofluorescence after mating for 30 minutes at the designated temperature. (A) At the permissive temperature (21°C) rescue and localization of FAP93 in all four cilia is expected and serves as a control. At the restrictive temperature (32°C; defective IFT) there are two possible results that will be indicative of the FAP93 assembly mechanism. If FAP93 is seen in all four cilia this will indicate that IFT is not required for assembly (B). If FAP93 requires IFT for assembly, FAP93 will only be seen on two cilia (C).

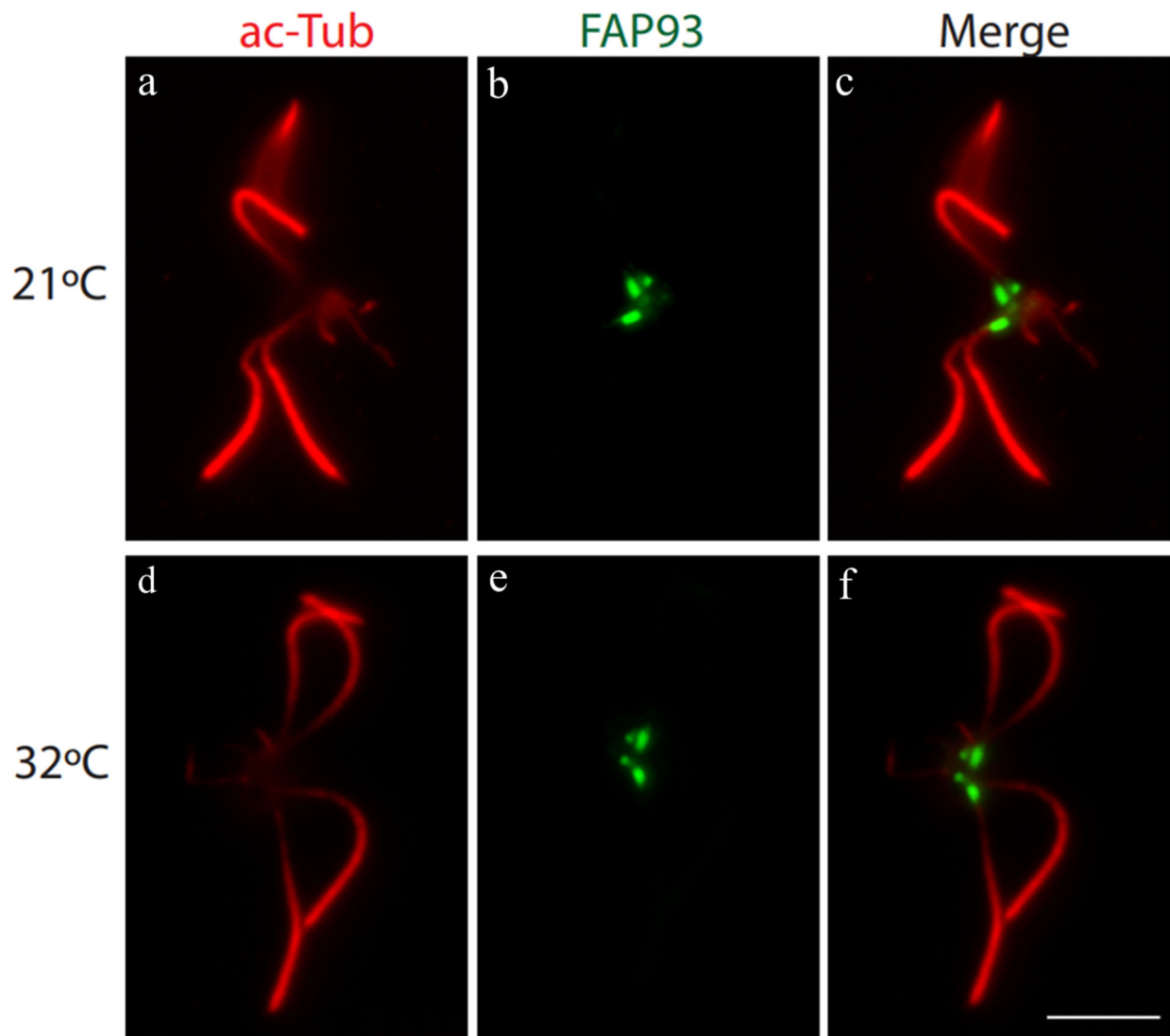


Figure 8. IFT is not required for FAP93 assembly in *fla10-1 x fap93;fla10-1* dikaryons.

The first column shows acetylated tubulin (ac-Tub) using a primary mouse monoclonal antibody 611B1 (a and d), ac-Tub is used to show the four cilia that indicate a dikaryon cell. FAP93 localization is observed in green (b and e). Dikaryons at both 21°C and 32°C show cells with four flagella indicating a dikaryon cell and four FAP93 stains indicating recovery of FAP93 (b, c, e, and f). The *fap93;fla10-1* FAP93 stains are smaller in size, indicating a partial rescue at both temperatures. The last column is a merged image of the two channels (c and f). (Scale bar = 10µm).

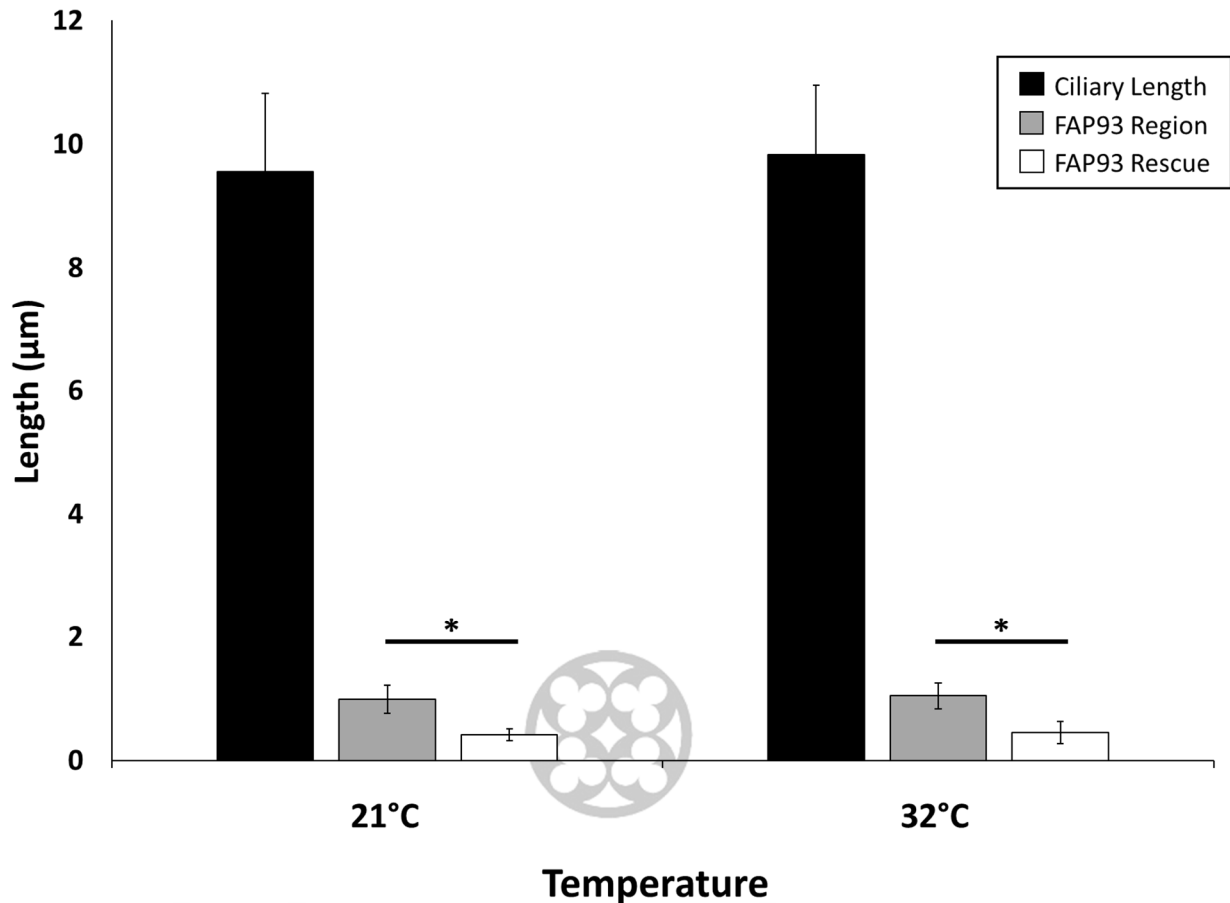


Figure 9. Dikaryon ciliary and FAP93 region length is similar and the FAP93 rescue is significantly different at both temperatures. Dikaryon ciliary length at 21°C was 9.55µm (±1.27µm), similarly at 32°C ciliary length was 9.83µm (±1.13µm). The FAP93 region refers to the wild-type sized region seen on *fla10-1* cilia and the FAP93 rescue region refers to the *fap93;fla10-1* FAP93 region. The FAP93 region at 21°C was 0.99µm (±0.23µm) and 1.05µm (±0.21µm) at 32°C, they were not significantly different. The FAP93 rescue region at 21°C was 0.42µm (±0.10µm) and 0.45µm (±0.18µm) at 32°C, not significantly different. At 21°C and at 32°C, the FAP93 region and FAP93 rescue region are significantly different than each other respectively. (p-value ≤ 0.001).

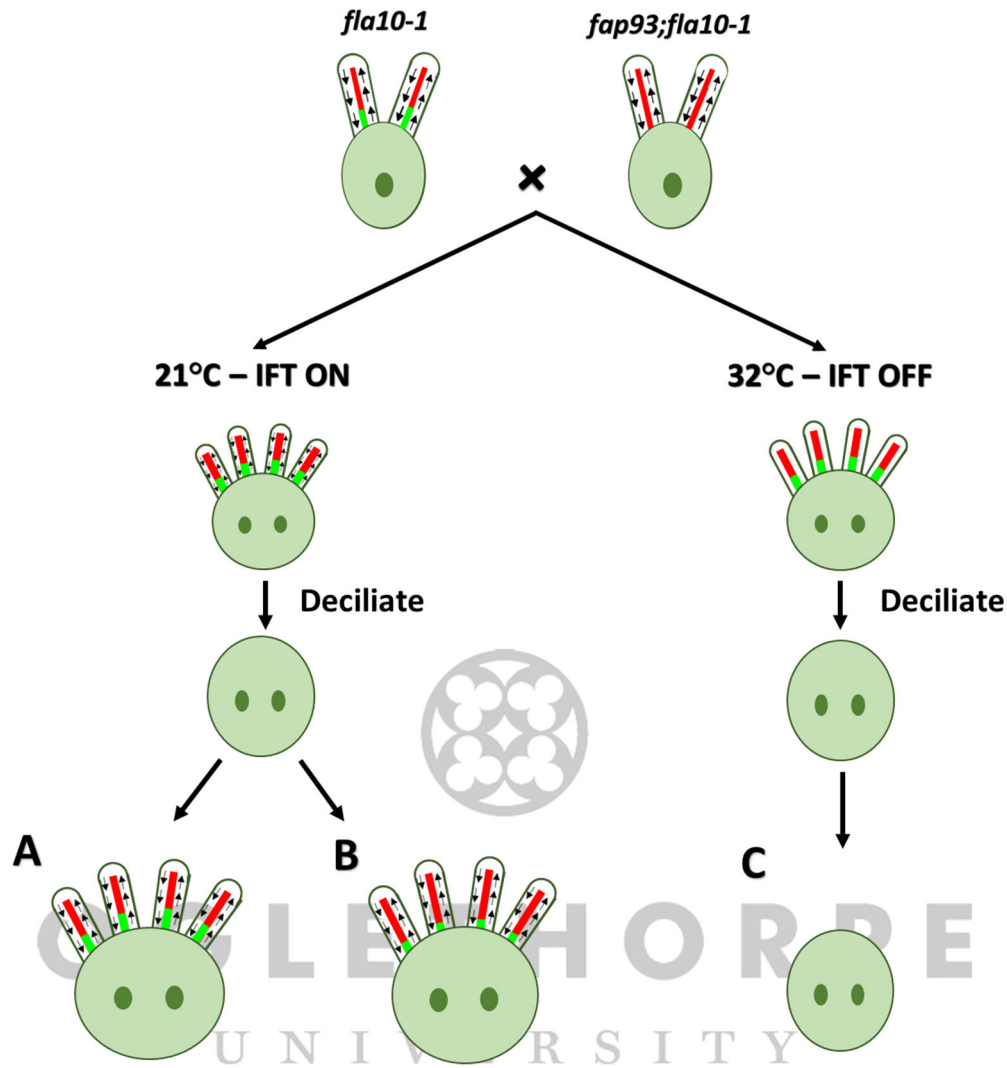


Figure 10. Experimental design of dikaryon rescue following deciliation to observe FAP93 while cilia are regenerating. Nitrogen starved cells are preincubated at either permissive (21°C) or restrictive (32°C) temperatures for 20 minutes. The cells are then mixed and allowed to mate for 30 minutes at the designated temperature. Following dikaryon formation, cells are deciliated and after an hour, once the cilia have regenerated, the cells are prepped for immunofluorescence. Antibodies for acetylated tubulin and FAP93 would be utilized to visualize the FAP93 rescue. On the left, when the cells are regenerated at the permissive temperature, two potential outcomes are depicted. In A, full rescue is depicted by four equal FAP93 regions that are wild-type size. In

B, partial rescue is depicted by four FAP93 regions of a smaller length. At the restrictive temperature shown on the right, IFT is off and these cells will not regenerate cilia, shown in **C**.

Deciliation at the restrictive temperature acts as an internal control to confirm IFT is off.

Methods

Cell Strains and Culture

Chlamydomonas reinhardtii strains used in this project were wild-type (CC-125) and, *fla10-1* (CC-1919) cells were obtained from the Chlamydomonas Cell Center. The *fap93;fla10-1* double mutant used was isolated by Susan Dutcher (Washington University, St. Louis) from tetrads following mating of the single mutants, *fla10-1* and *fap93*. Cells were grown at room temperature on L media plates placed above constant light. Cells were cultured in 300ml of L media with aeration for two to three days for analysis of vegetative cells. Cells used for dikaryon formation were inoculated in M-N media in 25mL conicals for two hours on a rotary wheel to starve cells of nitrogen and induce differentiation into gametes.

Dikaryon Formation at Permissive and Restrictive Temperatures

In conical tubes on a rotary wheel, 25mLs of *fla10-1* mating type (+) and *fap93;fla10-1* mating type (-) were starved of nitrogen in minimal media lacking nitrogen (M-N) at 21°C for two hours. The cells were analyzed via bright field microscopy to analyze cell health and test gamete mating. Following this step, each cell type was preincubated for 20 minutes at either 21°C or 32°C with no light to allow for the deactivation of the kinesin motors. After the preincubation the cells at each condition are mixed and allowed to mate for 30 minutes at either 21°C or 32°C with no light. Mating was seen in cells at both temperatures indicated by clustered cells apparently interacting with one another (Supplementary v.1 and v.2). Cells were collected by centrifugation

at 30, 60, or 90 or 120 minutes. After centrifugation for five minutes at 3000 rpm and 4°C, cells were prepped for immunofluorescence.

Immunofluorescence Microscopy

Cells were prepared for immunofluorescence microscopy using a fixation protocol for isolated cytoskeletons provided by Branch Craige (Craige et al., 2010) with modifications. Cells were washed with 5mL HMDEK (30mM HEPES, pH 7.4, 5mM MgSO₄, 1mM DTT, 0.5mM EGTA, and 25mM KCL) and spun down at 3000RPM for 5 minutes. The HMDEK is discarded and the cells are resuspended in 1mL HMDEK and 1mL of lysis buffer (2mL of 10% NP-40, 8mL of HMDEK, and 1 tablet of Roche protease inhibitor cocktail) and cells are kept on ice for 15 minutes. After lysis, 2mL of fixation buffer (1.25mL of 32% paraformaldehyde, 8.75 mL HMDEK) was added and the solution is then applied to coverslips to adhere for 15 minutes. The coverslips were then rinsed in 1X PBS and blocking solution (1% fish skin gellitin, 2% BSA, 15% horse serum, 0.02% saponin, 0.01% tritonx100 in pbs Ph 7.0) is applied for an hour. The block is then discarded, and the primary antibodies for acetylated tubulin and FAP93 are applied to the coverslip simultaneously to incubate overnight. After primary antibody incubation the cells were washed five times with block for a duration of five minutes each and then the secondary antibody was applied and incubated for one hour. Following the secondary incubation, the cells were washed five times with block for a duration of five minutes, rinsed off using PBS, and then mounted upon slides for imaging using Invitrogen ProLong Gold antifade mounting media. Images were acquired utilizing an Olympus epifluorescence imaging scope, using the Olympus cellsense software.

Antibodies

Primary antibodies used in this project included: mouse monoclonal antibody 611B1 (catalog #T7451) against acetylated tubulin and a rabbit monoclonal antibody against FAP93. Secondary antibodies used were anti-mouse-555 (catalog #A21422) and anti-rabbit-488 (catalog # A11008).

Images were analyzed in FIJI (Fiji is just image J).

Length analysis of cilia and FAP93 regions was performed using ImageJ FIJI software (Schindelin et al., 2012). Cells selected for length analysis were found at 100x magnification in the red channel to reduce bias and cells with more straight cilia were chosen. Olympus viewer images were taken in cellsense and opened as .oir files in FIGI using the OlympusViewer plugin. Files used contained metadata from microscope and the cellsense program, and the scale was confirmed manually with a stage micrometer for each analysis. Images were analyzed in one color channel using the line segment tool to trace the length of the cilia or FAP93 domain. All analysis have an N of over 40, and all statistical analysis was done via a two-tailed t-test. P-values less than 0.01 were considered significant.

References

- Alford LM, Mattheyses AL, Hunter EL, Lin H, Dutcher SK, Sale WS. 2013. The *Chlamydomonas* mutant pf27 reveals novel features of ciliary radial spoke assembly. Cytoskeleton (Hoboken). 70(12):804-818.
- Baker K, Beales PL. 2009. Making sense of cilia in disease: The human ciliopathies. Am J Med Genet C Semin Med Genet. 151C(4):281-295.
- Brown JM, Witman GB. 2014. Cilia and diseases. Bioscience. 64(12):1126-1137.
- Bui KH, Yagi T, Yamamoto R, Kamiya R, Ishikawa T. 2012. Polarity and asymmetry in the arrangement of dynein and related structures in the *Chlamydomonas* axoneme. J Cell

- Biol. 198(5):913-925.
- Cole DG. 2003. The intraflagellar transport machinery of *Chlamydomonas reinhardtii*. Traffic. 4(7):435-442.
- Cole DG, Diener DR, Himmelblau AL, Beech PL, Fuster JC, Rosenbaum JL. 1998. *Chlamydomonas* kinesin-ii-dependent intraflagellar transport (ift): Ift particles contain proteins required for ciliary assembly in caenorhabditis elegans sensory neurons. J Cell Biol. 141(4):993-1008.
- Craft JM, Harris JA, Hyman S, Kner P, Lechtreck KF. 2015. Tubulin transport by ift is upregulated during ciliary growth by a cilium-autonomous mechanism. J Cell Biol. 208(2):223-237.
- Craige B, Tsao CC, Diener DR, Hou Y, Lechtreck KF, Rosenbaum JL, Witman GB. 2010. Cep290 tethers flagellar transition zone microtubules to the membrane and regulates flagellar protein content. J Cell Biol. 190(5):927-940.
- Julie Craft Van De Weghe, J. Aaron Harris, Tomohiro Kubo, George B. Witman, Karl F. Lechtreck. 2020. Diffusion rather than intraflagellar transport likely provides most of the tubulin required for axonemal assembly in *Chlamydomonas*. J Cell Sci. 2020; 133 (17): jcs249805.
- Diener D. 2009. Analysis of cargo transport by ift and gfp imaging of ift in *Chlamydomonas*. Methods Cell Biol. 93:111-119.
- Dutcher SK. 2014. The awesome power of dikaryons for studying flagella and basal bodies in *Chlamydomonas reinhardtii*. Cytoskeleton (Hoboken). 71(2):79-94.
- Fliegauf M, Benzing T, Omran H. 2007. When cilia go bad: Cilia defects and ciliopathies. Nat Rev Mol Cell Biol. 8(11):880-893.

- Gibbons IR. 1981. Cilia and flagella of eukaryotes. *J Cell Biol.* 91(3 Pt 2):107s-124s.
- Harris JA, Liu Y, Yang P, Kner P, Lehtreck KF. 2016. Single-particle imaging reveals intraflagellar transport-independent transport and accumulation of eb1 in *Chlamydomonas* flagella. *Mol Biol Cell.* 27(2):295-307.
- Hoops HJ, Witman GB. 1983. Outer doublet heterogeneity reveals structural polarity related to beat direction in *Chlamydomonas* flagella. *J Cell Biol.* 97(3):902-908.
- Hunter EL, Lehtreck K, Fu G, Hwang J, Lin H, Gokhale A, Alford LM, Lewis B, Yamamoto R, Kamiya R et al. 2018. The ida3 adapter, required for intraflagellar transport of il dynein, is regulated by ciliary length. *Mol Biol Cell.* 29(8):886-896.
- Hwang, J., Yanagisawa, H., Davis, K.H., Hunter, E.L., Jimenez, A.R., Bower, R., Goodwin, R.E., Stuart, C.D.E., Dutcher, S.K., Porter, M.E., Sale, W.S., and Alford, L.M. Assembly of FAP93 at the proximal axoneme in *Chlamydomonas* cilia. Manuscript in preparation.
- King SM, Sale WS. 2018. Fifty years of microtubule sliding in cilia. *Mol Biol Cell.* 29(6):698-701.
- Kozminski KG, Beech PL, Rosenbaum JL. 1995. The *Chlamydomonas* kinesin-like protein fla10 is involved in motility associated with the flagellar membrane. *J Cell Biol.* 131(6 Pt 1):1517-1527.
- Kozminski KG, Johnson KA, Forscher P, Rosenbaum JL. 1993. A motility in the eukaryotic flagellum unrelated to flagellar beating. *Proc Natl Acad Sci U S A.* 90(12):5519-5523.
- Lehtreck KF. 2015. Ift-cargo interactions and protein transport in cilia. *Trends Biochem Sci.* 40(12):765-778.
- Lewis WR, Malarkey EB, Tritschler D, Bower R, Pasek RC, Porath JD, Birket SE, Saunier S, Antignac C, Knowles MR et al. 2016. Mutation of growth arrest specific 8 reveals a role

- in motile cilia function and human disease. PLoS Genet. 12(7):e1006220.
- Lucker BF, Behal RH, Qin H, Siron LC, Taggart WD, Rosenbaum JL, Cole DG. 2005. Characterization of the intraflagellar transport complex b core: Direct interaction of the ift81 and ift74/72 subunits. J Biol Chem. 280(30):27688-27696.
- Mitchell DR. 2007. The evolution of eukaryotic cilia and flagella as motile and sensory organelles. Adv Exp Med Biol. 607:130-140.
- Nicastro D. 2009. Cilia: Structure and motility. Methods in Cell Biology. 91:1-39.
- Nicastro D, Schwartz C, Pierson J, Gaudette R, Porter ME, McIntosh JR. 2006. The molecular architecture of axonemes revealed by cryoelectron tomography. Science. 313(5789):944-948.
- Oda T, Yanagisawa H, Kamiya R, Kikkawa M. 2014. A molecular ruler determines the repeat length in eukaryotic cilia and flagella. Science. 346(6211):857-860.
- Ostrowski LE, Dutcher SK, Lo CW. 2011. Cilia and models for studying structure and function. Proc Am Thorac Soc. 8(5):423-429.
- Pazour GJ, Agrin N, Leszyk J, Witman GB. 2005. Proteomic analysis of a eukaryotic cilium. J Cell Biol. 170(1):103-113.
- Pazour GJ, Witman GB. 2000. Forward and reverse genetic analysis of microtubule motors in *Chlamydomonas*. Methods. 22(4):285-298.
- Pigino G, Geimer S, Lanzavecchia S, Paccagnini E, Cantele F, Diener DR, Rosenbaum JL, Lupetti P. 2009. Electron-tomographic analysis of intraflagellar transport particle trains in situ. J Cell Biol. 187(1):135-148.
- Pigino G, Maheshwari A, Bui KH, Shingyoji C, Kamimura S, Ishikawa T. 2012. Comparative structural analysis of eukaryotic flagella and cilia from *Chlamydomonas*, *tetrahymena*,

- and sea urchins. *J Struct Biol.* 178(2):199-206.
- Piperno G, Mead K, Henderson S. 1996. Inner dynein arms but not outer dynein arms require the activity of kinesin homologue protein khp1(fla10) to reach the distal part of flagella in *Chlamydomonas*. *J Cell Biol.* 133(2):371-379.
- Piperno G, Ramanis Z. 1991. The proximal portion of *Chlamydomonas* flagella contains a distinct set of inner dynein arms. *J Cell Biol.* 112(4):701-709.
- Piperno G, Siuda E, Henderson S, Segil M, Vaananen H, Sassaroli M. 1998. Distinct mutants of retrograde intraflagellar transport (ift) share similar morphological and molecular defects. *J Cell Biol.* 143(6):1591-1601.
- Porter ME, Sale WS. 2000. The 9 + 2 axoneme anchors multiple inner arm dyneins and a network of kinases and phosphatases that control motility. *J Cell Biol.* 151(5):F37-42.
- Richey E, Qin H. 2013. Isolation of intraflagellar transport particle proteins from *Chlamydomonas reinhardtii*. *Methods Enzymol.* 524:1-17.
- Ringers C, Olstad EW, Jurisch-Yaksi N. 2020. The role of motile cilia in the development and physiology of the nervous system. *Philos Trans R Soc Lond B Biol Sci.* 375(1792):20190156.
- Rosenbaum JL, Cole DG, Diener DR. 1999. Intraflagellar transport: The eyes have it. *J Cell Biol.* 144(3):385-388.
- Rosenbaum JL, Witman GB. 2002. Intraflagellar transport. *Nat Rev Mol Cell Biol.* 3(11):813-825.
- Salomé PA, Merchant SS. 2019. A series of fortunate events: Introducing *Chlamydomonas* as a reference organism. *Plant Cell.* 31(8):1682-1707.
- Schindelin J, Arganda-Carreras I, Frise E, Kaynig V, Longair M, Pietzsch T, Preibisch S,

- Rueden C, Saalfeld S, Schmid B et al. 2012. Fiji: An open-source platform for biological-image analysis. *Nat Methods*. 9(7):676-682.
- Silflow CD, Lefebvre PA. 2001. Assembly and motility of eukaryotic cilia and flagella. Lessons from *Chlamydomonas reinhardtii*. *Plant Physiol*. 127(4):1500-1507.
- Stepanek L, Pigino G. 2016. Microtubule doublets are double-track railways for intraflagellar transport trains. *Science*. 352(6286):721-724.
- Szklarczyk D, Gable AL, Lyon D, Junge A, Wyder S, Huerta-Cepas J, Simonovic M, Doncheva NT, Morris JH, Bork P et al. 2018. String v11: Protein-protein association networks with increased coverage, supporting functional discovery in genome-wide experimental datasets. *Nucleic Acids Research*. 47(D1):D607–D613.
- Taschner M, Lorentzen E. 2016. The intraflagellar transport machinery. *Cold Spring Harb Perspect Biol*. 8(10).
- Tran NT, Kaldenhoff R. 2020. Achievements and challenges of genetic engineering of the model green alga *Chlamydomonas reinhardtii*. *Algal Research*. 50.
- Van der Heiden K, Egorova AD, Poelmann RE, Wentzel JJ, Hierck BP. 2011. Role for primary cilia as flow detectors in the cardiovascular system. *Int Rev Cell Mol Biol*. 290:87-119.
- Viswanadha R, Hunter EL, Yamamoto R, Wirschell M, Alford LM, Dutcher SK, Sale WS. 2014. The ciliary inner dynein arm, *ic1* dynein, is assembled in the cytoplasm and transported by *IFT* before axonemal docking. *Cytoskeleton (Hoboken)*. 71(10):573-586.
- Wallmeier J, Nielsen KG, Kuehni CE, Lucas JS, Leigh MW, Zariwala MA, Omran H. 2020. Motile ciliopathies. *Nat Rev Dis Primers*. 6(1):77.
- Walther Z, Vashishtha M, Hall JL. 1994. The *chlamydomonas fla10* gene encodes a novel kinesin-homologous protein. *J Cell Biol*. 126(1):175-188.

- Wang L, Dynlacht BD. 2018. The regulation of cilium assembly and disassembly in development and disease. *Development*. 145(18).
- Webb S, Mukhopadhyay AG, Roberts AJ. 2020. Intraflagellar transport trains and motors: Insights from structure. *Semin Cell Dev Biol*. 107:82-90.
- Wren KN, Craft JM, Tritschler D, Schauer A, Patel DK, Smith EF, Porter ME, Kner P, Lechtreck KF. 2013. A differential cargo-loading model of ciliary length regulation by ift. *Curr Biol*. 23(24):2463-2471.



O G L E T H O R P E
U N I V E R S I T Y